2014

The *Pseudomonas syringae* type III effector HopD1 suppresses effector-triggered immunity, localizes to the endoplasmic reticulum, and targets the Arabidopsis transcription factor NTL9

Anna Block
University of Nebraska - Lincoln

Tania Y. Toruno
University of Nebraska - Lincoln

Christian G. Elowsky
University of Nebraska-Lincoln, celowsky@unl.edu

Chi Zhang
University of Nebraska-Lincoln, zhang.chi@unl.edu

Jens Steinbrenner
University of Warwick

See last page for additional authors

New Phytologist

The *Pseudomonas syringae* type III effector HopD1 suppresses effector-triggered immunity, localizes to the endoplasmic reticulum, and targets the Arabidopsis transcription factor NTL9

Anna Block[1,2]*, Tania Y. Toruño[1,2]*, Christian G. Elowsky[3], Chi Zhang[1,4], Jens Steinbrenner[5], Jim Beynon[5] and James R. Alfano[1,2]

[1]Center for Plant Science Innovation, University of Nebraska, Lincoln, NE 68588-0660, USA; [2]Department of Plant Pathology, University of Nebraska, Lincoln, NE 68588-0722, USA; [3]Center for Biotechnology, University of Nebraska, Lincoln, NE 68588-0665, USA; [4]School of Biological Sciences, University of Nebraska, Lincoln, NE 68588-0118, USA; [5]School of Life Sciences, University of Warwick, Coventry CV4 7AL, UK

Author for correspondence:
James R. Alfano
Tel: +1 402 472 0395
Email: jalfano2@unl.edu

Received: *24 August 2013*
Accepted: *30 October 2013*

New Phytologist (2014) **201:** 1358–1370
doi: 10.1111/nph.12626

Key words: bacterial pathogens, plant defense, plant disease, plant immunity, type III effector.

Summary

- *Pseudomonas syringae* type III effectors are known to suppress plant immunity to promote bacterial virulence. However, the activities and targets of these effectors are not well understood.
- We used genetic, molecular, and cell biology methods to characterize the activities, localization, and target of the HopD1 type III effector in Arabidopsis.
- HopD1 contributes to *P. syringae* virulence in Arabidopsis and reduces effector-triggered immunity (ETI) responses but not pathogen-associated molecular pattern-triggered immunity (PTI) responses. Plants expressing HopD1 supported increased growth of ETI-inducing *P. syringae* strains compared with wild-type Arabidopsis. We show that HopD1 interacts with the membrane-tethered Arabidopsis transcription factor NTL9 and demonstrate that this interaction occurs at the endoplasmic reticulum (ER). A *P. syringae hopD1* mutant and ETI-inducing *P. syringae* strains exhibited enhanced growth on Arabidopsis *ntl9* mutant plants. Conversely, growth of *P. syringae* strains was reduced in plants expressing a constitutively active NTL9 derivative, indicating that NTL9 is a positive regulator of plant immunity. Furthermore, HopD1 inhibited the induction of NTL9-regulated genes during ETI but not PTI.
- HopD1 contributes to *P. syringae* virulence in part by targeting NTL9, resulting in the suppression of ETI responses but not PTI responses and the promotion of plant pathogenicity.

Introduction

The Gram-negative bacterial pathogen *Pseudomonas syringae* pv. *tomato* DC3000 is the causative agent of bacterial speck disease on tomato and pathogenic on the model plant *Arabidopsis thaliana*. One of its primary virulence factors is its ability to inject type III effector (T3E) proteins into host cells using a type III protein secretion system. Once injected, T3Es target and disrupt various host processes in order to suppress plant immunity (Block & Alfano, 2011; Deslandes & Rivas, 2012; Feng & Zhou, 2012).

Plant innate immunity can be broadly separated into two branches based on how microorganism recognition is achieved. The first of these branches involves the recognition of pathogen-associated molecular patterns (PAMPs) by extracellular pattern recognition receptors (PRRs; Jones & Dangl, 2006). This recognition induces multiple responses, including signaling cascades involving mitogen-activated protein kinases and calcium-dependent protein kinases. These signaling events lead to a rapid burst of reactive oxygen species (ROS) production and gene expression changes (Monaghan & Zipfel, 2012). Later responses include cell wall modifications such as the deposition of callose. The combined response arising from this recognition event is termed PAMP-triggered immunity (PTI; Jones & Dangl, 2006; Monaghan & Zipfel, 2012).

Pseudomonas syringae can use several of its injected T3Es to suppress PTI and achieve high growth rates within its host plants. To combat PTI suppression by T3Es and other pathogen effectors, plants evolved a second layer of immunity based on the recognition of effectors or their activities by plant immune receptors, know as resistance (R) proteins. The response from this recognition event is termed effector-triggered immunity (ETI) and induces many of the same responses as PTI but often with different timing and amplitude (Tsuda & Katagiri, 2010). ETI is

*These authors contributed equally to this work.

usually associated with a form of programmed cell death known as the hypersensitive response (HR). Thus, in order to maintain its pathogen status, *P. syringae* probably adapted/evolved T3Es to suppress PTI and/or ETI.

If a *P. syringae* strain lacks the ability to successfully suppress ETI, bacterial growth is restricted. This is classically referred to as an incompatible interaction between an avirulent strain and a resistant plant (Keen, 1990). If the *P. syringae* strain can suppress PTI and ETI, or does not elicit ETI but suppresses PTI, it can be pathogenic and achieve high growth rates in plant tissue. This is classically referred to as a compatible interaction between a virulent strain and susceptible plant. Many *P. syringae* T3Es have been shown to suppress PTI responses and several suppress both PTI and ETI (Block *et al.*, 2008; Gimenez-Ibanez & Rathjen, 2010; Feng & Zhou, 2012). However, it is less clear whether *P. syringae* T3Es have evolved to suppress ETI, but not PTI.

In a previous study we screened DC3000 T3Es for their ability to suppress ETI responses induced by the T3E HopA1 in *Nicotiana tabacum* (Jamir *et al.*, 2004; Guo *et al.*, 2009). One of the strong ETI suppressors identified in this screen was HopD1. HopD1 is a homolog of AvrPphD from *P. syringae* pv. *phaseolicola* race 4 strain 1302A (Wood *et al.*, 1994). A *P. syringae* pv. *phaseolicola avrPphD* mutant showed no difference in growth in either resistant or susceptible pea cultivars, indicating that its immune suppression/induction functions are probably redundant with other T3Es in this pathogen (Arnold *et al.*, 2001). Bacterial mutants lacking HopD1 homologs have differing effects on the virulence of other bacterial pathogens (Guo *et al.*, 2002; Schulze *et al.*, 2012). Therefore, depending on the pathogen and its likely redundancy with other T3Es, loss of *hopD1* can reduce the virulence of a pathogen.

HopD1 has no known mechanism of action or homology to proteins with a known enzymatic function. A recent study used a high-throughput yeast two-hybrid screen to define the interactomes of *P. syringae* T3Es and the effectors from the oomycete pathogen *Hyaloperonospora arabidopsidis* with Arabidopsis proteins (Mukhtar *et al.*, 2011). One potential interaction identified in this screen was that of HopD1 and the Arabidopsis NTL9 (At4g35580) protein (Mukhtar *et al.*, 2011). NTL9 belongs to the NAC with Transmembrane Motif 1 (NTM1)-like family of transcription factors that are tethered to intracellular membranes (Kim *et al.*, 2006). NAC transcription factors play a wide variety of roles in developmental and stress-related signaling and can also be involved in regulating cross-talk between different stresses (Puranik *et al.*, 2012).

Here we show that HopD1 is an important DC3000 virulence factor. We show that it is a strong ETI suppressor in Arabidopsis but does not significantly suppress PTI responses. Additionally, we confirm that HopD1 interacts with NTL9 and that both HopD1 and NTL9 localize to the plant endoplasmic reticulum (ER). NTL9 is important for the Arabidopsis ETI response as *ntl9* knockout plants allow for increased growth of ETI-inducing *P. syringae* strains and rescue the growth of a DC3000 *hopD1* mutant. In addition, plants expressing constitutively active *NTL9* are more resistant to virulent and ETI-inducing *P. syringae* strains, further indicating that NTL9 is a positive regulator of plant immunity. We identify several genes whose expression is induced by active NTL9 and show that HopD1 suppresses the induction of these genes during ETI but not PTI. These data indicate that HopD1 functions as a specific suppressor of ETI, in part by inhibiting NTL9-mediated gene expression.

Materials and Methods

Cloning and expression constructs

Genes were cloned into the Gateway entry vector pENTR-D. The pENTR-D constructs and their respective cloning primers are as follows: *hopD1* with a ribosome binding site (pLN3228) primers P0967 (5′-CACCGGGACAGCTGATAGAACAATGA ATCCTCTACGCTC-3′) and P2892(5′-GGGTGCGGGCT GCCGCGA-3′); *hopD1* (pLN5056) primers P4373 (5′-CACC ATGAATCCTCTACGATCTATTCAACAC-3′) and P2892; *NTL9* (pLN5057) primers P4379 (5′-CACCATGGGTGCTGT ATCGATGGAGTCG-3′) and P4393 (5′-TGAACTCACCAG TGTCCTCCACATCC-3′); and $NTL9_{1\text{-}330}$ (pLN5058) primers P4379 and P4382 (5′-GAAAGCCATGAAGTCGTTGAAAGC ATCCTCTG-3′).

For the *hopD1* bimolecular fluorescence complementation (BiFC) constructs, *hopD1* with a 3′ *XhoI* restriction site was amplified with primers P4373 and P4384 (5′-GATCCTCGAG GGGTGCGGGCTG CCGCGACGTG-3′); *cyfp* with a 5′ *XhoI* restriction site was amplified with primers P4342 (5′-GATCCTC GAGATGGACAAGCAGAAGAACGGCATC-3′ – which contains an ATG start codon) and P4343 (5′-TCAGATAGATC TCTTGTACAGCTC-3′); and *nyfp* with a 5′ *XhoI* restriction site was amplified with primers P4340 (5′-GATCCTCGAGATGG TGAGCAAGGG CGAGGAG-3′) and P4341 (5′-TCAGGCCA TGATATAGACGTTGTGG). The PCR products were then digested with *XhoI* and ligated. The ligation products were used as templates to clone *hopD1-cyfp* with primers P4373 and P4343 into pENTR-D, resulting in the construct pLN5066, and *hopD1-nyfp* with primers P4373 and P4341 into pENTR-D, resulting in the construct pLN5067. For the *NTL9* BiFC constructs, *NTL9* with a 5′ *XhoI* restriction site was amplified with primers P4403 (5′-GATCCTCGAGATGGTGCTGTATCGAT GGAGTCG-3′) and P4393; *cyfp* with a 3′ *XhoI* restriction site was amplified with primers P4406 (5′-CACCATGGACAAGCA AGCAGAAGAACGGCATC-3′) and P4407 (5′-GATCCTCGA GGATAGATCTCTTGTACAGCTC-3′); and *nyfp* with a 3′ *XhoI* restriction site was amplified with primers P4404 (5′-CACC ATGGTGAGCAAGGCGAGGAG-3′) and P4405 (5′-GATCC TCGAGGGCCTGATATAGACGTTGTGG-3′). The PCR products were then digested with *XhoI* and ligated. The ligation products were used as templates to clone *nyfp-NTL9* with primers P4404 and P4393 into pENTR-D, resulting in the construct pLN5068, and *cyfp-NTL9* with primers P4406 and P4393 into pENTR-D, resulting in the construct pLN5069.

The BiFC clones pLN5066, pLN5067, pLN5068 and pLN5069 were placed into the plant constitutive expression vector pLN462 (Jamir *et al.*, 2004), resulting in constructs

pLN5070, pLN5071, pLN5072 and pLN5073, respectively. For plant expression, *hopD1* (pLN5056) was fused to a C-terminal hemagglutinin (HA) tag by recombining into pLN462 with gateway technologies to give pLN5060 and to a C-terminal green fluorescent protein (GFP) tag by recombining into pK7FWG2 (Karimi *et al.*, 2002) to give pLN5061. For complementation of the *hopD1* mutant (UNL104), *hopD1* (pLN3228) was recombined into the Tn7 vector pLN2992 (Choi *et al.*, 2005), resulting in construct pLN4908. This vector was then used to insert the resultant *hopD1-ha* into the chromosome of UNL104. To create an N-terminal GFP fusion to NTL9, pLN5057 was recombined with pK7WGF2 (Karimi *et al.*, 2002) to give pLN5062. To make an estradiol-inducible $NTL9_{1\text{-}330}$-HA, pLN5058 was recombined with the gateway-compatible pER8 vector pLN604 (Zuo *et al.*, 2000) to give pLN5063.

Pathogenicity assays

Pseudomonas syringae strains were grown overnight at 30°C on King's B (KB; King *et al.*, 1954) media with the appropriate antibiotics and resuspended to an OD_{600} of 0.2 (2×10^8 cells ml^{-1}) in 10 mM $MgCl_2$. Cells were serially diluted in 10 mM $MgCl_2$ to the appropriate cell density and infiltrated into the fully expanded leaves of 4-wk-old *Arabidopsis thaliana* Col-0 wild-type, mutant, and/or transgenic plants using a needleless syringe. Plants were kept at 100% humidity and 1 cm^2 leaf disks were sampled at the indicated times, ground in 10 mM $MgCl_2$, serially diluted and plated on KB agar plates. Plates were incubated for 48 h at 30°C and number of cells cm^{-2} was determined. Four to six leaf disks were sampled for each treatment and the statistical significance of the resulting data was analyzed by one-way ANOVA.

HR and ion leakage

Pseudomonas fluorescens (*Pf*)(pLN1965), *Pf*(pLN1965 + p*avrRpm1*) and *Pf*(pLN1965 + p*avrRpm1* + p*hopD1-flag*; Guo *et al.*, 2009) were grown overnight at 30°C in KB media with appropriate antibiotics. Bacterial strains were resuspended at 1×10^8 cells ml^{-1} in 5 mM 2-(4-morpholino)-ethane sulfonic acid (MES), pH 5.6. Wild-type Arabidopsis (Col-0) and *rpm1* mutant (Eitas *et al.*, 2008) leaves were infiltrated with bacterial suspensions using a needleless syringe. Nine leaf disks were harvested for each strain in each plant type using a 0.7 cm^2 cork borer. Three leaf disks were placed in each 15 ml polypropylene tube with 5 ml of water and incubated in a shaker for 30 min at room temperature. Water was removed and 5 ml of fresh water was added to each sample and tubes were placed in a shaker. Electrolyte leakage was monitored at the indicated time points using an electrical conductivity meter (Fisher Scientific, Pittsburgh, PA, USA). Conductivity was measured in µS cm^{-1}. For macroscopic HR, *Pf*(pLN1965 + p*avrRpm1*) and *Pf* (pLN1965 + p*avrRpm1* + p*hop D1-flag*) strains were infiltrated into leaves of wild-type Arabidopsis (Col-0) and the *rpm1* mutant at 1×10^8 cells ml^{-1} using a needleless syringe. Leaves were photographed 2 d after infiltration.

Callose assay

Wild-type (Col-0) and HopD1-HA transgenic lines were syringe-infiltrated with 10 µM flg22, or wild-type Arabidopsis leaves were syringe-inoculated with 1×10^6 cells ml^{-1} of *Pf* (pLN1965), *Pf*(pLN1965 + *hopD1-flag*), *Pf*(pLN1965 + p*avrRpm1*) or *Pf*(pLN1965 + p*avrRpm1* + *hopD1-flag*). Sixteen hours later, leaves were harvested and cleared with 100% (v/v) ethanol at 37°C for 4 h and washed twice with 70% (v/v) ethanol and three times with water. The completely cleared leaves were stained with 0.1% (w/v) aniline blue in a solution of 150 mM K_2HPO_4, pH 9.5, for 30 min and the callose deposits were enumerated as in Block *et al.* (Block *et al.*, 2010).

Oxidative burst measurement

Leaf disks of 0.5 cm^2 were cut from wild-type (Col-0) and HopD1-HA transgenic lines and floated on 0.1 ml of water in wells of a 96-well plate for 16 h in the dark. The water was then removed and replaced with 0.5 mM L-012 (Wako, Japan) in 10 mM MES buffer, pH 7.4. For PAMP treatment, 1 µM of flg22, elf18 or chitin was added to the buffer. The rate of ROS production was determined by counting photons from L-012-mediated chemiluminescence using a luminometer (Asai *et al.*, 2008). The rates of ROS production were calculated as the number of photons released in 30 min after treatment with photons counted once a minute.

Yeast-two hybrid

Gateway entry constructs carrying *hopD1* (pLN5056) and *NTL9* (pLN5057) were recombined by an LR reaction to the appropriate yeast two-hybrid destination vectors to generate pDEST-DB::*hopD1* (pLN4988) and pDEST-AD::*NTL9* (pLN4970). A detailed protocol for the yeast-two hybrid analysis used is described in Dreze *et al.* (2010). The yeast strains Y8930 (MATα) and Y8800 (MAT**a**) were transformed with expression plasmids pDEST-DB:;*hopD1* and pDEST-AD:;*NTL9*, respectively. Empty expression vectors (EVs) were also transformed into the corresponding yeast strains. Yeast Y8930 (pDEST-DB::*hopD1* or EV) was mated to Y8800 (pDEST-AD::*NTL9* or EV) in a mating plate (yeast extract peptone dextrose). Growth was checked on Sc-Leu-Trp and interactions were tested by plating mated strains in Sc-Leu-Trp-His + 1 mM 3-amino-1,2,4-triazole (3AT).

Agroinfiltration and confocal microscopy

Agrobacterium strains were coinfiltrated into *N. benthamiana* as in Block *et al.* (2010). Leaves were imaged 48 h later using a Nikon A1 confocal mounted on an Eclipse 90i Nikon compound microscope using the following excitation (ex) and emission (em) wavelengths: GFP and yellow fluorescent protein (YFP), 488 nm (ex), 500–550 nm (em); red fluorescent protein (RFP), 561.5 nm (ex) and 570–620 nm (em); Chl, 641 nm (ex) and 662–737 nm (em). Dual color image acquisition was sequential.

Semiquantitative reverse transcription polymerase chain reaction (RT-PCR)

Wild-type Arabidopsis (Col-0) and pER8 NTL9$_{1\text{-}330}$-HA stable Arabidopsis lines were syringe-infiltrated with 0.2 mM estradiol or a water control. Leaf tissue was harvested for RNA extraction 24 h after treatment. Wild-type Arabidopsis (Col-0) plants were syringe-inoculated with water or 1×10^7 cells ml^{-1} of *Pf* (pLN1965 + p*avrRpm1*) or *Pf*(pLN1965 + p*avrRpm1* + p*hopD1-flag*). Leaf tissue was harvested for RNA extraction 4 h after infiltration. Total RNA was purified using RNeasy mini Kit with on-column DNase treatment (Qiagen). The reverse transcription of RNA was carried out using RETROscript (Ambion) using oligo(dT) primers with heat denaturation of the RNA. *actin2* (At3g18780) was used as a reference gene with primers P3774 (5′-GCACTTGTGTGTGACAAACTCTCTGG-3′) and P3775 (5′-GGCATCAATTCGATCACTCTAGAGC-3′). The following gene-specific primers were used to measure expression levels in quantitative (qRT-PCR): *HAB1* (*At1g72770*) P4556 (5′-GCG GTGATTCGAGGGCGGTTT-3′) and P4557 (5′-GCCACGT TTGTGTGATGTGCATT-3′); *NIP2* (*At2g17730*) P4558(5′-T CTTCAGGATTTCCAGCTCGGTGAA-3′) and P4559 (5′-C GGGCAAGAACCGTGTCTAAGGA-3′); *ADF6* (*At2g31200*) P4560 (5′-TTGCTTGGTCTCCTTCGACCTCTGG-3′) and P4561 (5′-TCTCAGTTCGCTCGTTCGCGT-3′); *PAL1* (*At2 g37040*) P3922 (5′-AGCAGCAAGAGCAGCCTACGAT AA-3′) and P3923 (5′-TGTTCCAAGCTCTTCCCTCACGA A-3′); *FRK1* (*At2g19190*) P4476 (5′-ACCCCGAGTACTATT CGACTCGCCA-3′) and P4477 (5′-TGAGCTTGCAATAGC AGGTTGGCCT-3′); and *NHL10* (*At2g35980*) P4562 (5′-TCA CTGTTCCTGTCCGTAACCCAA-3′) and P4563 (5′-TGGTA CTAAACCGCTTTCCTCGT-3′). qRT-PCR was run using IQ™ SYBR® Green supermix (BioRad) on a BioRad iCycler. Gene expression relative to Col-0 was calculated using $2^{-\Delta\Delta C_T}$ with *actin2* as the reference gene and mock-treated Col-0 as the reference sample.

Additional information on the methods used for the data presented in the supporting information can be found in Supporting Information, Methods S1.

Results

HopD1 contributes to *P. syringae* virulence and enhances the growth of ETI-inducing *P. syringae* strains

To determine the extent of HopD1's involvement in *P. syringae* virulence, we measured the *in planta* growth of a *P. syringae* pv. *tomato* DC3000 *hopD1* mutant (UNL104; Jamir *et al.*, 2004) in wild-type Arabidopsis (Col-0; Fig. 1a). Bacterial growth assays showed a slight but significant reduction in the growth of the *hopD1* mutant in Arabidopsis when compared with wild-type DC3000. Wild-type growth rates were restored when *hopD1* was reintroduced into the *hopD1* mutant using a T7 expression system such that *hopD1* was expressed in single copy from a type III promoter (Fig. 1a). These data show that HopD1 is required for the full virulence of *P. syringae* on Arabidopsis.

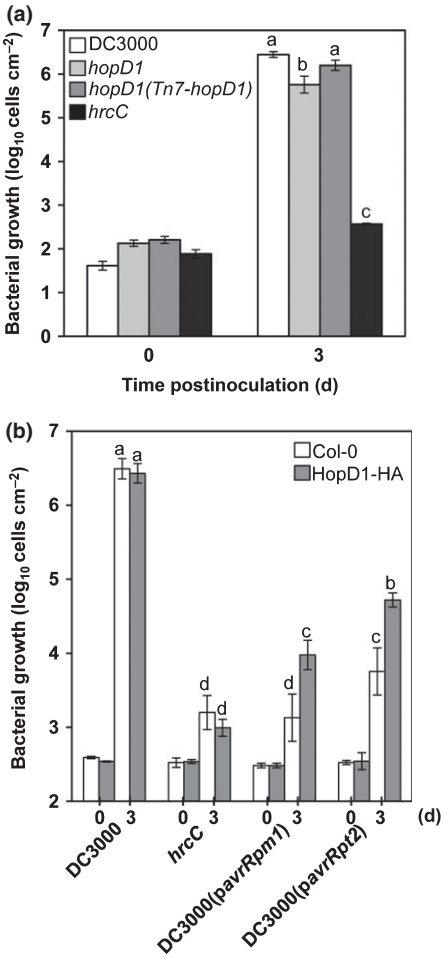

Fig. 1 HopD1 contributes to the virulence of DC3000. (a) Wild-type Arabidopsis (Col-0) plants were syringe-inoculated with 2×10^5 cells ml^{-1} of wild-type *Pseudomonas syringae* (DC3000), the DC3000 *hopD1* mutant or the *hopD1* mutant complemented with *hopD1-flag* using the Tn7 expression system. The type III secretion defective *hrcC* mutant was included as a nonpathogenic control. Bacterial growth was determined at 0 and 3 d postinoculation (letters are significantly different, $P \leq 0.05$). (b) Wild-type Arabidopsis (Col-0) and transgenic Arabidopsis constitutively expressing HopD1-HA were syringe-inoculated with 2×10^5 cells ml^{-1} of DC3000, DC3000 carrying a plasmid constitutively expressing the *avr* genes *avrRpm1* or *avrRpt2*, or the DC3000 *hrcC* mutant. Bacterial growth was measured at 0 and 3 d postinoculation (different letters indicate the values are significantly different; $P \leq 0.05$). (a, b) Error bars, ± SE.

Next we examined the ability of HopD1 to promote bacterial growth *in planta* using transgenic Arabidopsis constitutively expressing HopD1 fused to a C-terminal HA tag (HopD1-HA). These plants displayed no obvious phenotypes and we confirmed that they produced HopD1-HA (Fig. S1). Wild-type Arabidopsis and HopD1-HA expressing Arabidopsis plants were syringe-inoculated with wild-type DC3000, the DC3000 *hrcC* mutant defective in type III secretion, or DC3000 strains carrying plasmids expressing the T3E genes *avrRpm1* or *avrRpt2*, which encode ETI-inducing T3Es, rendering these strains avirulent. Growth of these strains was determined at 0 and 3 d postinoculation (Fig. 1b). *In planta* expression of HopD1-HA led to significantly increased growth of the two ETI-inducing avirulent strains

but had no effect on the growth of wild-type DC3000 or the nonpathogenic *hrcC* mutant (Fig. 1b). These data show that HopD1 is a strong suppressor of ETI in Arabidopsis. The lack of an effect of HopD1 on the growth of the *hrcC* mutant, which cannot inject T3Es but carries PAMPs that induce PTI, suggests that HopD1 is unable to significantly suppress PTI.

Bacterially delivered HopD1 can suppress AvrRpm1-induced ETI in Arabidopsis

The increased growth of avirulent *P. syringae* strains on Arabidopsis expressing HopD1-HA indicates that HopD1 can suppress ETI induced by AvrRpm1 and AvrRpt2 in Arabidopsis. To further characterize the ability of HopD1 to suppress ETI, we used a nonpathogenic *Pf* strain carrying pLN1965, which encodes a functional *P. syringae* type III secretion system (Guo *et al.*, 2009), and two additional plasmids expressing HopD1-FLAG and AvrRpm1. This allows the effect of HopD1 on ETI to be determined in the absence of other T3Es that may be redundant to HopD1.

To test the ability of HopD1 to suppress ETI, *Pf* (pLN1965 + p*avrRpm1*) carrying either a vector control or a plasmid constitutively expressing *hopD1-flag* were syringe-infiltrated into wild-type Arabidopsis leaves. The coexpression of *hopD1-flag* with *avrRpm1* suppressed the macroscopic HR (Fig. 2a). AvrRpm1-induced ion leakage was also measured in wild-type Col-0 infiltrated with these strains. Bacterial delivery of HopD1-FLAG suppressed ion leakage, which is correlated with cell death, to such an extent that it resembled that of leaves infiltrated with *Pf* lacking the ETI inducer AvrRpm1 (Fig. 2b). Furthermore, the ETI-induced deposition of callose in the plant cell wall of wild-type Arabidopsis leaves infiltrated with *Pf*(pLN1965 + p*avrRpm1* + p*hopD1-flag*) was significantly lower than that in leaves infiltrated with *Pf*(pLN1965 + p*avrRpm1*; Fig. 2c). These data show that HopD1 can suppress ETI-induced HR and callose deposition.

To confirm that the HR and ion leakage suppression by HopD1 was the result of suppression of ETI, we included an Arabidopsis *rpm1* knockout line that cannot recognize AvrRpm1 and, therefore, does not exhibit AvrRpm1-induced ETI responses. Using this Arabidopsis *rpm1* mutant, there was no induction of an HR by either *Pf*(pLN1965 + p*avrRpm1*) or *Pf* (pLN1965 + p*avrRpm1* + p*hopD1-flag*) and there was no difference in ion leakage (Fig. S2). Collectively, these data confirm that HopD1 can suppress AvrRpm1-induced ETI responses in Arabidopsis.

HopD1 does not suppress PAMP-induced oxidative burst or callose deposition in Arabidopsis

To determine if HopD1 could suppress PTI, we evaluated its ability to inhibit the oxidative burst that occurs within minutes of PAMP recognition (Nanda *et al.*, 2010). To do this, we measured the production of ROS in wild-type and HopD1-HA-expressing Arabidopsis after treatment with the PTI inducers flg22, elf18, and chitin. Flg22 is a 22-amino-acid peptide of the

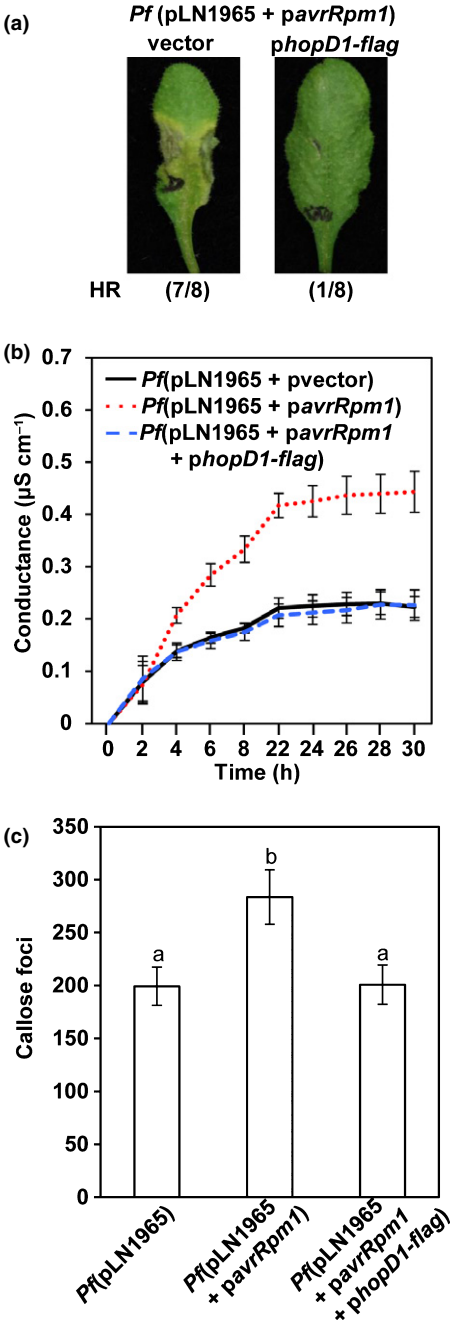

Fig. 2 HopD1 suppresses effector-triggered immunity (ETI) in Arabidopsis. Wild-type Arabidopsis (Col-0) plants were syringe-inoculated with 1×10^8 cells ml^{-1} of *Pseudomonas fluorescens* (*Pf*)(pLN1965), which encodes a functional type III secretion system, and a construct carrying *avrRpm1* (*Pf*(pLN1965 + p*avrRpm1*)), carrying a vector control (*Pf* (pLN1965 + pvector)), or carrying *avrRpm1* and a plasmid constitutively expressing *hopD1-flag* (*Pf*(pLN1965 + p*avrRpm1* + p*hopD1-flag*)). (a) The hypersensitive response (HR) was scored in eight leaves per treatment at 48 h postinoculation. (b) Ion leakage was measured in leaf disks over time to quantify cell death. (c) Wild-type Arabidopsis (Col-0) leaves were syringe-inoculated with 1×10^6 cells ml^{-1} of *Pf*(pLN1965) or *Pf*(pLN1965) carrying *avrRpm1* with or without a plasmid constitutively expressing *hopD1-flag* and the number of callose foci were determined at 16 h postinoculation (different letters indicate that values are significantly different; $P \leq 0.05$). Each assay was repeated at least twice with similar results. (b, c) Error bars, ± SE.

PAMP flagellin that is recognized by the plant receptor FLS2 and elf18 is an 18-amino-acid peptide of the PAMP EF-Tu that is recognized by the receptor EFR. The PAMP chitin is recognized by the receptor CERK1 (Monaghan & Zipfel, 2012). No difference was observed in PAMP-induced ROS production between wild-type and HopD1-HA-expressing Arabidopsis, indicating that HopD1 cannot suppress this early PTI response (Fig. 3a).

If HopD1 targets an intermediate stage in PTI signaling, it may suppress later PTI responses without altering ROS production. Therefore, we measured the ability of HopD1 to suppress PAMP-induced callose deposition, a late PTI response (Nicaise *et al.*, 2009), in wild-type and HopD1-HA expressing Arabidopsis plants treated with flg22. No difference in flg22-induced callose deposition was observed between wild-type Arabidopsis and Arabidopsis expressing HopD1-HA (Fig. 3b). To confirm this lack of PTI suppression, we measured the extent that bacterially delivered HopD1 could suppress PAMP-induced callose deposition in response to recognition of *Pf* PAMPs. To do this, wild-type Arabidopsis was infiltrated with *Pf*(pLN1965) carrying a vector control or a plasmid constitutively expressing *hopD1-flag*.

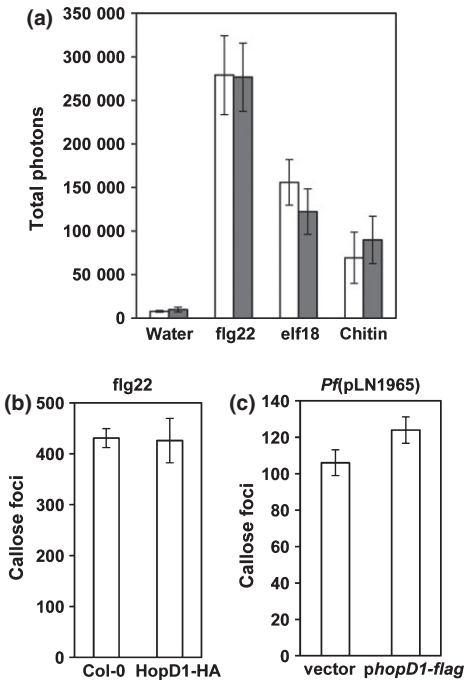

Fig. 3 HopD1 has no significant impact on pathogen-associated molecular pattern (PAMP)-induced reactive oxygen species (ROS) production or callose deposition in Arabidopsis. (a) Leaf disks were taken from wild-type Arabidopsis (Col-0; open bars) and transgenic Arabidopsis constitutively expressing HopD1-HA (closed bars) and were treated with water or the PAMPs flg22, elf18, or chitin. ROS production was measured for 30 min after treatment by quantifying luminescence of the luminol derivative L-012. (b) Callose deposition was determined in wild-type and HopD1-HA-expressing Arabidopsis in response to flg22 treatment. (c) Callose deposition was determined in wild-type Arabidopsis (Col-0) syringe-inoculated with *Pf*(pLN1965) containing either a vector control or a plasmid constitutively expressing *hopD1-flag*. Bacterial delivery of HopD1-FLAG had no effect on the production of callose in response to *Pseudomonas fluorescens* (*Pf*)(pLN1965) treatment. Each experiment was repeated at least twice with similar results and ± SE is indicated.

No difference in PAMP-induced callose deposition as a result of the bacterial delivery of HopD1 was observed (Fig. 3c). These data suggest that while HopD1 is a strong suppressor of ETI, it has no detectable effect on these PTI responses. Therefore, it is likely that HopD1 suppresses ETI-specific components of plant immunity.

HopD1 interacts with the membrane-tethered Arabidopsis transcription factor NTL9

A high-throughput yeast-two-hybrid screen that defined the *P. syringae* effector interactome with Arabidopsis proteins identified the Arabidopsis membrane-tethered NAC transcription factor NTL9 as a possible interactor for HopD1 (Mukhtar *et al.*, 2011). Three splice variants have been identified for *NTL9* owing to differential splicing of its fourth intron. Splice variant 1 is the only one with a C-terminal transmembrane domain. RT-PCR analyses with primers flanking the fourth intron of *NTL9* were used to differentiate between splice variant 1 and splice variants 2 and 3 during biotic stress. We performed RT-PCR using these primers with RNA isolated from untreated Arabidopsis and Arabidopsis treated with *Pf*(pLN1965 + p*avrRpm1*) or *Pf* (pLN1965 + p*avrRpm1* + p*hopD1-flag*). In all treatments, splice variant 1 was the only form observed, indicating that it is the dominant form of this gene in these conditions (Fig. S3).

As the interaction between NTL9 and HopD1 was identified using a yeast two-hybrid screen, we first confirmed this interaction by cloning *hopD1* and *NTL9* into yeast two-hybrid system vectors. Yeast strains expressing both *hopD1* and *NTL9* grew on selective media while *hopD1* and *NTL9* with their respective empty vector controls did not, confirming the interaction between HopD1 and NTL9 in yeast (Fig. 4a).

The interaction of two proteins in yeast does not necessarily translate into an interaction *in planta*. To confirm their interaction *in planta*, BiFC was performed. *Nicotiana benthamiana* was co-agroinfiltrated with NTL9 fused at its N-terminus to the N-terminal half of YFP and HopD1 fused at its C-terminus to the C-terminal half of YFP. Infiltrated leaves were examined with confocal microscopy and yellow fluorescence was observed in cells of the infiltrated leaves (Fig. 4b), indicating that these proteins interacted *in planta*. The reciprocal experiment with HopD1 fused at its C-terminus to the N-terminal half of YFP and NTL9 fused at its N-terminus to the C-terminal half of YFP also produced yellow fluorescence (Fig 4b). No yellow fluorescence was observed in leaves infiltrated with BiFC HopD1 or NTL9 constructs and their corresponding nYFP or cYFP controls (Fig 4b). These data indicate that HopD1 interacts with NTL9 *in planta*.

HopD1 and NTL9 localize to the plant endoplasmic reticulum

The reticulate pattern in the cytoplasm accompanied by a distinct ring around the nucleus observed in the BiFC experiments involving HopD1 and NTL9 is characteristic of ER-localized proteins. To investigate whether HopD1 and/or NTL9 localized

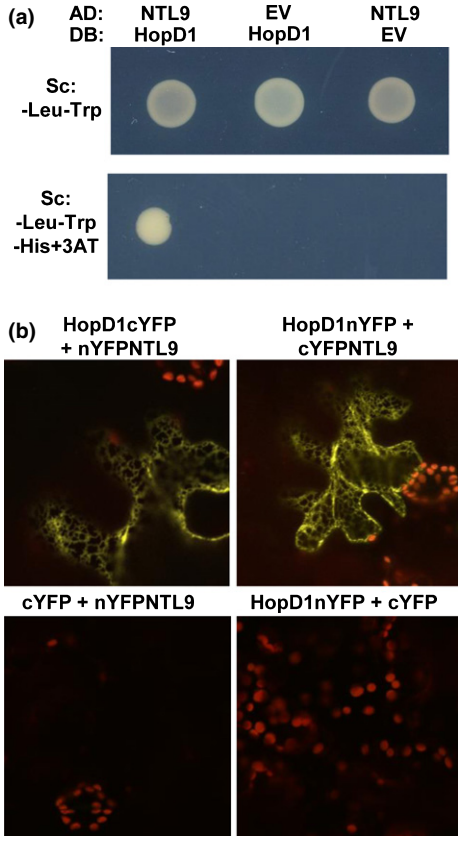

Fig. 4 HopD1 interacts with the membrane-tethered Arabidopsis transcription factor NTL9. (a) Yeast-two-hybrid analysis of HopD1 and NTL9 shows growth on selective media (Sc:-Leu-Trp-His + 1 mM 3AT) when both HopD1 and NTL9 are present. (b) Bimolecular fluorescence complementation (BiFC) analysis of HopD1 and NTL9 interactions in *Nicotiana benthamiana* cells. HopD1-cYFP and nYFP-NTL9 and HopD1-nYFP and cYFP-NTL9 were expressed in *N. benthamiana* using *Agrobacterium*-mediated transient expression. Yellow fluorescence indicates that yellow fluorescent protein (YFP) moieties are in close proximity to each other. Red fluorescence represents Chl autofluorescence. No YFP fluorescence was seen in coinfiltration experiments of *hopD1* and *NTL9* BiFC constructs with the respective cYFP control.

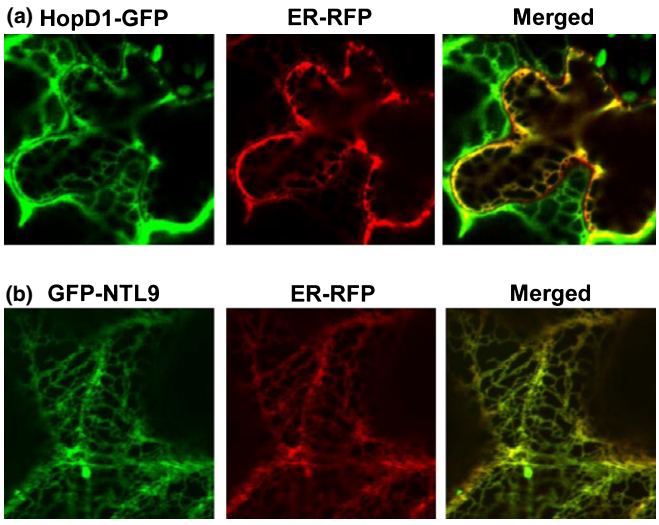

Fig. 5 HopD1 and NTL9 localize to the plant endoplasmic reticulum (ER). (a) *Agrobacterium*-mediated transient expression of a C-terminal fusion of HopD1 to green fluorescent protein (GFP) (green) (HopD1-GFP) and an ER-localized mCherry (red) fused at its N-terminus with the signal peptide from AtWAK2 and at its C-terminus with the ER retention signal (ER-RFP) in *Nicotiana benthamiana* was visualized using confocal microscopy. (b) *Agrobacterium*-mediated transient expression of NTL9 with an N-terminal GFP fusion (GFP-NTL9) and ER-localized mCherry reporter in *N. benthamiana* and visualized using confocal microscopy.

to the plant ER, we performed colocalization experiments with a known ER marker. DNA encoding the ER-localized RFP marker CD3-960 (Nelson *et al.*, 2007) was agroinfiltrated into *N. benthamiana* with DNA encoding either HopD1 fused at its C-terminus to GFP or NTL9 fused at its N-terminus to GFP, both under the control of a constitutive CaMV 35S promoter. Confocal microscopy revealed colocalization of HopD1-GFP with ER-RFP (Fig. 5a) and GFP-NTL9 with ER-RFP (Fig. 5b). These data indicate that both HopD1 and NTL9 are localized to the ER in *N. benthamiana*. The most likely orientation for NTL9 is with its C-terminal transmembrane domain inserted in the ER membrane with a minor portion of NTL9 in the ER lumen and the majority of the protein in the cytoplasm. Membrane-tethered transcription factors are held in a ready state in the membrane and upon activation are cleaved at the cytoplasmic side of the transmembrane domain, releasing an active transcription factor that can enter the nucleus and regulate transcription (Kim *et al.*, 2006). The protease that performs this cleavage for NTL9 has not been identified. The localization of HopD1 and NTL9 to the ER and their interaction at this site as indicated in BiFC experiments suggests that HopD1 is targeting NTL9 while it is anchored in the ER membrane.

NTL9 is involved in the Arabidopsis immune response to *P. syringae*

As HopD1 is a strong suppressor of ETI, it stands to reason that if it targets NTL9, NTL9 is likely a component of plant immunity. An emerging theme for NAC transcription factors is their multiple roles in biotic and abiotic stress, as well as an ability to coordinate multiple stress responses (Puranik *et al.*, 2012). This has been seen for the membrane-tethered NAC transcription factor NTL6 that coordinates the response to cold and pathogen attack as it up-regulates pathogenesis-related genes (Seo *et al.*, 2010). A loss-of-function line for *NTL9* (SALK-065051, *ntl9-1*) was isolated that is compromised in osmotic stress responses and has enhanced susceptibility to avirulent *Hyaloperonospora arabidopsidis* (Yoon *et al.*, 2008; Mukhtar *et al.*, 2011), suggesting that NTL9 is involved in the response to both osmotic and pathogen stresses.

To investigate the role of NTL9 in the response of Arabidopsis to *P. syringae*, wild-type Arabidopsis and the Arabidopsis *ntl9-1* mutant were syringe-inoculated with various *P. syringae* strains and bacterial growth was measured at 0 and 3 d postinoculation (Fig. 6a). DC3000 grew to equivalent levels in wild-type and *ntl9-1* Arabidopsis, as did the *hrcC* mutant. Interestingly, the reduced growth of the *hopD1* mutant observed in wild-type

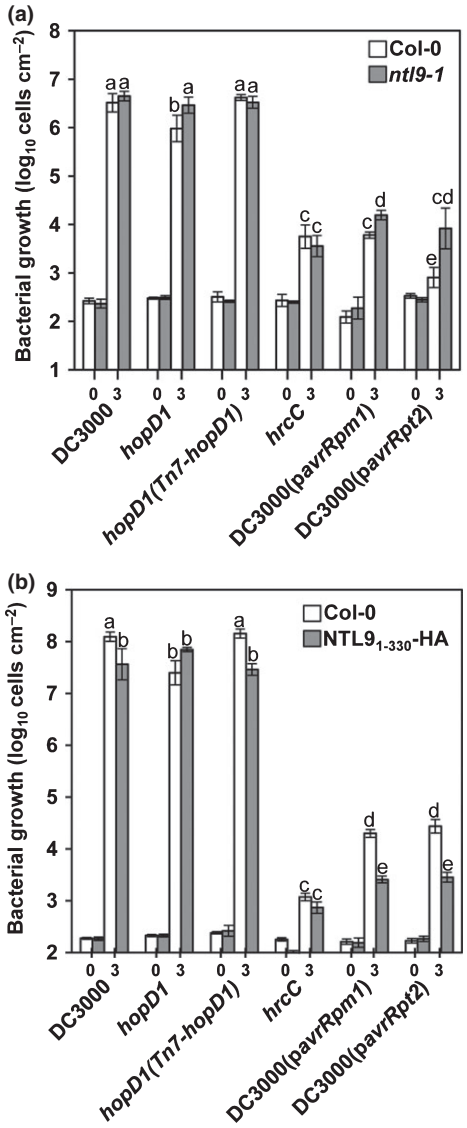

Fig. 6 NTL9 is important for the innate immune response of Arabidopsis to *Pseudomonas syringae*. (a) Wild-type Arabidopsis (Col-0) and the *ntl9* knockout mutant (*ntl9-1*) were syringe-inoculated with 2×10^5 cells ml^{-1} of wild-type *P. syringae* (DC3000), the *hopD1* mutant, *hopD1* complemented using the Tn7 expression system (*hopD1(Tn7-hopD1)*), the type III secretion defective *hrcC* mutant, and avirulent *P. syringae* strains DC3000(p*avrRpt2*) and DC3000(p*avrRpm1*). Bacterial growth was measured at 0 and 3 d postinoculation. (b) Wild-type Arabidopsis (Col-0) and transgenic plants expressing constitutively active NTL9 (*$NTL9_{1-330}$-HA*) under the control of an estradiol-inducible promoter were sprayed with 20 μM estradiol and syringe-inoculated 24 h later with 2×10^5 cells ml^{-1} of DC3000, *hopD1*, *hopD1(Tn7-hopD1)*, *hrcC*, DC3000 (p*avrRpt2*) or DC3000(p*avrRpm1*). Bacterial growth was measured at 0 and 3 d postinoculation. (a, b) These experiments were repeated three times with similar results (different letters indicate that the values are significantly different; $P \leq 0.05$). Error bars, ± SE.

Arabidopsis plants was restored to DC3000 values in *ntl9-1* mutant plants. These data support the hypothesis that NTL9 is a target of HopD1. As expected, the DC3000 *hopD1* mutant complemented with *hopD1* showed equivalent growth to DC3000 in both wild-type and *ntl9-1* mutant plants. The avirulent *P. syringae* strains DC3000(p*avrRpm1*) and DC3000(p*avrRpt2*) showed enhanced growth in Arabidopsis *ntl9-1* mutant plants compared with wild-type Arabidopsis, indicating that NTL9 is involved in ETI. These results are consistent with our earlier results (Figs 1b, 2), indicating that HopD1 targets components of immunity associated with ETI.

A truncated version of NTL9 that consisted of amino acids 1–330 ($NTL9_{1-330}$) is constitutively active (Yoon *et al.*, 2008). We made transgenic Arabidopsis lines expressing *$NTL9_{1-330}$-HA* under the control of an estradiol-inducible promoter. Wild-type and *$NTL9_{1-330}$-HA*-expressing Arabidopsis were sprayed with estradiol to induce transgene expression. Twenty-four hours later the plants were syringe-inoculated with 2×10^5 cells ml^{-1} of various *P. syringae* strains and bacterial growth was measured at 0 and 3 d postinoculation (Fig. 6b). Growth of both DC3000 and the complemented DC3000 *hopD1* mutant were reduced to that of the *hopD1* mutant in plants expressing activated *NTL9*. In addition, growth of the avirulent *P. syringae* strains was also reduced in the *$NTL9_{1-330}$-HA*-expressing lines. These data show that active NTL9 up-regulates plant immunity resulting in the restriction of *P. syringae* growth *in planta*.

Identification of NTL9-induced genes involved in plant immunity

If HopD1 functions by inhibiting NTL9's activity during ETI, it would be likely that HopD1 suppresses NTL9-dependent gene expression during ETI. NTL9 has been shown to regulate several genes involved in abiotic stress (Yoon *et al.*, 2008), yet its regulation of genes involved in plant immunity is not well understood. To determine if NTL9 could regulate the expression of a subset of genes associated with immunity, *FRK1*, *PAL1*, and *NHL10* expression was measured using qRT-PCR in wild-type and $NTL9_{1-330}$-HA-inducible Arabidopsis with and without estradiol treatment (Fig. 7a). The expression of all three immunity-related genes was induced exclusively in the estradiol-treated $NTL9_{1-330}$-HA plants showing that they are up-regulated either directly or indirectly by active NTL9. Because of the extensive overlap between ETI and PTI (Tsuda & Katagiri, 2010), we do not know if the expression of these genes represents an ETI or a PTI response in this experiment.

In a previous study, Kim *et al.* used PCR-mediated random binding site selection to identify the sequence TTGCTTANNNNNNAAG as the DNA-binding site for NTL9 (Kim *et al.*, 2007a). We used this binding site to search for additional NTL9-regulated Arabidopsis genes using RSA-tools-dna-pattern search (http://rsat.ulb.ac.be/genome-scale-dna-pattern_form.cgi; van Helden *et al.*, 2000). In all, 175 Arabidopsis genes were identified with the binding site motif in their promoter within 1 kb of their predicted translational start site. We selected 20 of these 175 genes for further analysis based on their possible role in innate immunity. Their possible involvement in immunity was established via literature searches or as a result of induction of their expression by DC3000 treatment according to the microarray database Arabidopsis eFP Browser (http://www.bar.utoronto.ca/efp/cgi-bin/efpWeb.cgi; Winter *et al.*, 2007).

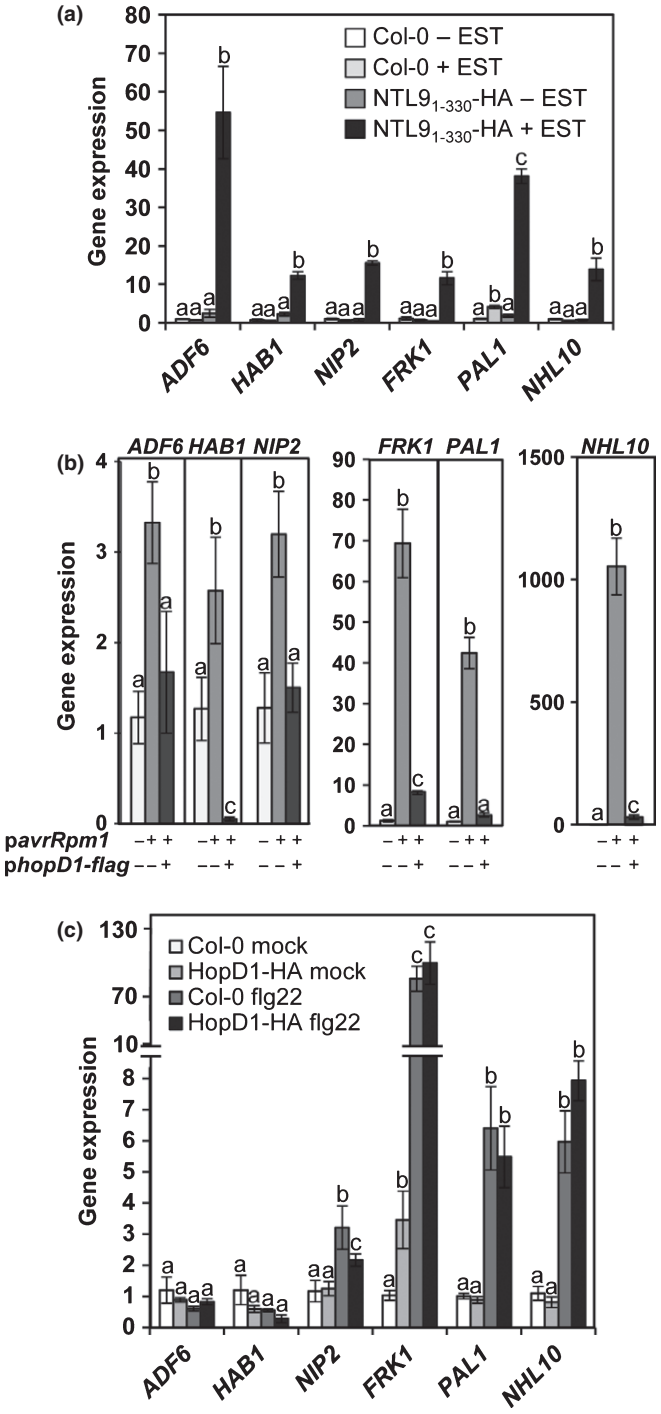

Fig. 7 HopD1 suppresses effector-triggered immunity (ETI) but not pathogen-associated molecular pattern (PAMP)-induced NTL9-regulated genes. (a) Wild-type (Col-0) and transgenic Arabidopsis expressing a constitutively active NTL9 derivative (NTL9$_{1-330}$-HA) under the control of an estradiol (EST)-inducible promoter were syringe-infiltrated with EST or a mock control. Leaf tissue was sampled 24 h later and gene expression was analyzed by quantitative reverse transcription polymerase chain reaction (qRT-PCR). (b) Wild-type (Col-0) Arabidopsis plants were syringe-inoculated with a mock control or 1×10^7 cells ml^{-1} of *Pseudomonas fluorescens* (*Pf*)(pLN1965 + p*avrRpm1*) with an empty vector control or with a plasmid constitutively expressing HopD1-FLAG. Inoculated leaves were sampled 4 h later and gene expression was measured using qRT-PCR. Expression of the genes was increased in response to the ETI-inducer AvrRpm1 only in the absence of HopD1. (c) Wild-type (Col-0) and HopD1-HA-expressing Arabidopsis were syringe-infiltrated with 1 μM flg22 or a mock control. Infiltrated leaves were sampled 4 h later and gene expression was measured using qRT-PCR. Induction of gene expression by flg22 was not significantly altered by the presence of HopD1. In all experiments, expression is relative to untreated Col-0. (a–c) Different letters indicate the values are significantly different using ANOVA ($P \leq 0.05$); error bars, ± SE.

Expression of the 20 candidate genes was measured by qRT-PCR in wild-type Arabidopsis and NTL9$_{1-330}$-HA-inducible plants with and without estradiol treatment (Table S1). Owing to the limited number of base pairs in the predicted binding site, the false positive rate was high and many of the genes tested did not show NTL9-regulated expression (Table S1). Despite this high error rate, four of the predicted genes were strongly up-regulated in estradiol-treated NTL9$_{1-330}$-HA-inducible lines. These genes were *ADF6* (*At2g31200*), *NIP2* (*At2g17730*), *HAB1* (*At1g72770*) (Fig. 7a) and *BZIP9* (*At5g24800*) (Table S1).

HopD1 suppresses NTL9-regulated gene expression during ETI but not PTI

In order to investigate HopD1's ability to suppress NTL9's function in ETI, the expression of NTL9-regulated genes was measured in wild-type Arabidopsis plants infiltrated with a mock control, *Pf*(pLN1965 + p*avrRpm1*) or *Pf*(pLN1965 + p*avrRpm1* + p*hopD1-flag*). One of the genes tested (*BZIP9*) was repressed by *Pf*(pLN1965 + p*avrRpm1*) treatment (Fig. S4). The other six genes showed increased expression upon AvrRpm1-induced ETI and little if any increase in expression by AvrRpm1 in the presence of HopD1 (Fig. 7b). *FRK1* is known primarily to be associated with PTI. However, it is induced during AvrRpm1-induced ETI (Fig. 7b). These data suggest that HopD1 inhibits ETI-induction of NTL9-regulated gene expression and, therefore, it interferes with NTL9 function during ETI.

Because HopD1 specifically blocks ETI and not PTI responses, we examined the ability of HopD1 to affect the expression of the six NTL9-regulated marker genes during PTI. To accomplish this, wild-type and HopD1-HA-expressing Arabidopsis were syringe-infiltrated with flg22 or a mock control. Leaf tissue was sampled 4 h later and gene expression was measured using qRT-PCR (Fig. 7c). Three of the six genes, *FRK1*, *PAL1* and *NHL10*, showed induction in response to flg22 treatment. However, the presence of HopD1-HA had no effect on the PTI induction of these genes. Thus, taken together, these data indicate that NTL9 is specifically involved in the ETI induction of immunity-related gene expression and the induction of a subset of these genes during PTI is probably controlled by other transcription factors.

Discussion

In this study we examined the role of the HopD1 T3E in the virulence of the bacterial pathogen *P. syringae*. Baltrus *et al.* (2011) found that HopD1 was a well-distributed T3E, which was found

in all sequenced strains of group I, two-thirds of the sequenced group III strains, and none of the six sequenced group II strains. We found that HopD1 was necessary for the full virulence of *P. syringae* (Fig. 1a) and that it was a strong suppressor of ETI (Fig. 2), but apparently not of PTI. The extent to which transgenically expressed HopD1 was capable of PTI suppression was evaluated with three commonly used PTI assays: the *in planta* growth of a *P. syringae hrcC* mutant (Fig. 1b), defective in type III secretion, or a nonpathogenic *P. fluorescens* strain (Fig. 3c); PAMP-induced ROS production (Fig. 3a); and PAMP-induced callose deposition (Fig. 3b). However, we did not test the extent to which HopD1 allowed better *P. syringae* growth in plants pretreated with a PAMP, which would be an additional assay to evaluate PTI suppression. Nevertheless, based on these commonly used PTI assays, it seems likely that HopD1 is not an effective PTI suppressor.

We found that HopD1 interacts with the NAC transcription factor NTL9 and both localize to the ER of plants (Figs 4, 5). The growth of the *P. syringae hopD1* mutant and ETI-inducing *P. syringae* strains was enhanced in an Arabidopsis *ntl9* mutant (Fig. 6a), while expression of constitutively active *NTL9* suppressed the growth of both virulent and ETI-inducing *P. syringae* strains (Fig. 6b). This indicates that NTL9 is utilized in the Arabidopsis innate immune response to *P. syringae*. In addition, we observed that HopD1 suppressed ETI-induced but not PAMP-induced expression of NTL9-regulated genes (Fig. 7). Collectively, these data led us to conclude that HopD1 suppresses ETI and promotes virulence of *P. syringae* in part by blocking the ability of NTL9 to regulate ETI-induced gene expression.

HopD1 was shown previously to suppress the HopA1-induced HR in tobacco (Jamir *et al.*, 2004; Guo *et al.*, 2009). The ability of HopD1 to suppress ETI in two different systems (tobacco and Arabidopsis) and in response to multiple recognized T3Es (HopA1, AvrRpm1 and AvrRpt2) indicates that one of its primary targets is a common component of ETI. Interestingly, we did not find any evidence that HopD1 suppressed PTI. The specific effect of HopD1 on ETI suggests that the reduced virulence of the *hopD1* mutant exhibited in Arabidopsis is probably the result of an 'unmasking' of recognized *P. syringae* T3Es owing to the loss of HopD1's ETI suppression activity. Earlier reports provided pioneering genetic evidence suggesting that *avr* genes, encoding recognized T3Es, can reside in virulent *P. syringae* strains and can be 'unmasked' when other T3E genes, encoding ETI suppressors, are mutated (Jackson *et al.*, 1999; Tsiamis *et al.*, 2000). Moreover, Arabidopsis mutants with defective R protein complexes allow for enhanced growth of a virulent *P. syringae* strain (Zhang *et al.*, 2010), consistent with ETI playing an immunity role against virulent *P. syringae*. Our research further supports that ETI contributes to immunity against virulent *P. syringae* and that HopD1 disables ETI as a virulence strategy.

The coevolution of plants and pathogens is elegantly illustrated in the zigzag model of the plant immune system (Jones & Dangl, 2006). In this coevolutionary model, PRRs recognize PAMPs inducing PTI. To retain pathogenicity the pathogen must acquire or evolve an effector that can suppress PTI, resulting in effector-triggered susceptibility (ETS). Therefore, the earliest T3Es used in *P. syringae* virulence are predicted to be PTI suppressors. In the next phase, the plant evolves an R protein to recognize a specific pathogen effector, thereby inducing ETI. This would put selection pressure on the pathogen to disable the gene encoding the recognized effector or acquire another effector to suppress the ETI evoked from this recognition event, allowing the return of ETS. Importantly, the ability for the pathogen to regain ETS is probably dependent on its inventory of effectors that can suppress ETI and the strength of the ETI response induced by the recognized effector. *P. syringae* T3Es have been investigated mostly for their effect on PTI (Feng & Zhou, 2012). However, there are several examples of *P. syringae* T3Es that suppress both PTI and ETI (Abramovitch *et al.*, 2003; Gohre *et al.*, 2008; Gimenez-Ibanez *et al.*, 2009; Wang *et al.*, 2010; Wilton *et al.*, 2010). This is perhaps not surprising given the highly overlapped nature of PTI and ETI (Tsuda *et al.*, 2008). What is less common are examples of *P. syringae* T3Es that suppress ETI but not PTI. These effectors would be predicted to be acquired later in the coevolution of the pathogen–plant interaction after establishment of the R protein immune receptor surveillance system. HopD1 appears to be one such effector.

We clearly show by yeast two-hybrid and BiFC assays that HopD1 interacts with NTL9. GFP fusions of both of these proteins colocalize with an ER-targeted RFP fusion and BiFC assays show that HopD1 and NTL9 interact at the ER. NTL9 was previously reported to localize to the plasma membrane and nucleus of onion cells (Yoon *et al.*, 2008). The large vacuole of onion cells that oppresses the ER against the plasma membrane, coupled with the difficulty in distinguishing nuclear and perinuclear localization with epifluorescence microscopy, may have led to these observed differences in localization.

NTL9 is one of over 110 NAC domain transcription factors in Arabidopsis (Ooka *et al.*, 2003), of which at least 13 have C-terminal transmembrane domains (Kim *et al.*, 2007b). There is precedent for pathogens to target NAC transcription factors, arguably the most well characterized of which is the capsid protein (CP) of *Turnip crinkle virus* (TCV) that interacts with the Arabidopsis NAC transcription factor TIP (Ren *et al.*, 2000), blocking its ability to localize to the nucleus (Ren *et al.*, 2005). We tested the extent to which HopD1 could affect the subcellular localization of NTL9 using *Agrobacterium*-mediated transient assays in *N. benthamiana* of GFP-NTL9 with or without HopD1-HA and were unable to discern any difference in GFP-NTL9 localization (Fig. S5). However, based on these results, DC3000 can induce the relocalization of NTL9-GFP to the nucleus in *N. benthamiana*. Additionally, we tested whether HopD1 was able to inhibit NTL9 transcription using a yeast one-hybrid system and were unable to detect a decrease in transcription in the presence of HopD1 (Fig. S6). Thus, HopD1 inhibits NTL9-dependent gene expression, but we do not yet know the mechanism of its inhibition.

NAC transcription factors have also been implicated in the plant immune response to bacterial pathogens. For example, the plasma membrane-bound Arabidopsis NAC transcription factor NTL6 has been implicated in the cold induction of innate immunity as a constitutively active form of NTL6 activates the

expression of the pathogenesis-related genes *PR1*, *PR2* and *PR5* (Seo *et al.*, 2010). Arabidopsis plants constitutively expressing active NTL6 are more resistant to *P. syringae*, and NTL6 RNAi lines are more susceptible to *P. syringae* after cold pretreatment (Seo *et al.*, 2010). Another NAC transcription factor from Arabidopsis, ATAF1, is a negative regulator of immune responses against *P. syringae* (Wang *et al.*, 2009).

Relatively recently a report showed that *ntl9* knockout Arabidopsis plants are subtly more resistant to *P. syringae* (Kim *et al.*, 2012). These data led the authors to suggest that NTL9 is a negative regulator of innate immunity. However, we did not observe any statistically significant difference in the growth of *P. syringae* in *ntl9* knockout plants compared with wild-type plants and often observed a slight increase in *P. syringae* growth (Fig. 6a), even though these experiments were repeated many times. Importantly, Arabidopsis plants expressing constitutively active *NTL9* were more resistant to *P. syringae* (Fig. 6b), which suggests that NTL9 acts as a positive regulator. We cannot account for the differences between our *P. syringae* growth phenotypes and that reported in Kim *et al.* (2012). However, their subtle *P. syringae* growth data and our own data suggest that the absence of NTL9 may be compensated for by other transcription factors in plant immunity.

Our study shows that NTL9 induces the classic immune marker genes *FRK1* (He *et al.*, 2006), *PAL1* (Mishina & Zeier, 2007) and *NHL10* (Zipfel *et al.*, 2004), as well as at least three genes that have not been characterized as to their role in innate immunity. These genes are *HAB1*, *NIP2* and *ADF6*. NIP2 has no known role in immunity. Although no direct role for ADF6 has been shown in the immune response to *P. syringae* infection, another actin-depolymerizing factor (ADF4) was shown to be specifically required for resistance triggered by the *P. syringae* effector AvrPphB (Tian *et al.*, 2009). HAB1 is a negative regulator of ABA signaling. It is a 2C protein phosphatase that, in the absence of ABA, binds to SnRK2 kinases, inhibiting their activity (Soon *et al.*, 2012). ABA has a negative role in plant immunity (Cao *et al.*, 2011) and it would not be surprising, therefore, if the induction of a negative regulator of ABA signaling, such as HAB1, by NTL9 was important for immunity signaling. Other ETI-associated genes are also likely to be regulated by NTL9, but their identification will require extensive NTL9-dependent expression studies, which will be addressed in the future. Other future studies will examine HopD1's effect on NTL9 and other NAC transcription factors during pathogen stress, which will help to elucidate how this T3E inhibits the function of NTL9 as well as understanding the role NTL9 plays in plant immunity.

Acknowledgements

We would like to thank the Alfano group members for fruitful discussions and comments regarding this manuscript. We would also like to thank Dr Ed Cahoon for the vector CD3-96. The research was supported by grants to J.R.A. from the US Department of Agriculture (award no. 2007-35319-18336) and the National Institutes of Health (award no. 1R01AI069146-01A2).

References

Abramovitch RB, Kim YJ, Chen S, Dickman MB, Martin GB. 2003. *Pseudomonas* type III effector AvrPtoB induces plant disease susceptibility by inhibition of host programmed cell death. *EMBO Journal* **22**: 60–69.

Arnold DL, Gibbon MJ, Jackson RW, Wood JR, Brown J, Mansfield JW, Taylor JD, Vivian A. 2001. Molecular characterization of *avrPphD*, a widely-distributed gene from *Pseudomonas syringae* pv. *phaseolicola* involved in non-host recognition by pea (*Pisum sativum*). *Physiological and Molecular Plant Pathology* **58**: 55–62.

Asai S, Ohta K, Yoshioka H. 2008. MAPK signaling regulates nitric oxide and NADPH oxidase-dependent oxidative bursts in *Nicotiana benthamiana*. *Plant Cell* **20**: 1390–1406.

Baltrus DA, Nishimura MT, Romanchuk A, Chang JH, Mukhtar MS, Cherkis K, Roach J, Grant SR, Jones CD, Dangl JL. 2011. Dynamic evolution of pathogenicity revealed by sequencing and comparative genomics of 19 *Pseudomonas syringae* isolates. *PLoS Pathogens* **7**: e1002132.

Block A, Alfano JR. 2011. Plant targets for *Pseudomonas syringae* type III effectors: virulence targets or guarded decoys? *Current Opinion in Microbiology* **14**: 39–46.

Block A, Guo M, Li G, Elowsky C, Clemente TE, Alfano JR. 2010. The *Pseudomonas syringae* type III effector HopG1 targets mitochondria, alters plant development and suppresses plant innate immunity. *Cellular Microbiology* **12**: 318–330.

Block A, Li G, Fu ZQ, Alfano JR. 2008. Phytopathogen type III effector weaponry and their plant targets. *Current Opinion in Plant Biology* **11**: 396–403.

Cao FY, Yoshioka K, Desveaux D. 2011. The roles of ABA in plant-pathogen interactions. *Journal of Plant Research* **124**: 489–499.

Choi KH, Gaynor JB, White KG, Lopez C, Bosio CM, Karkhoff-Schweizer RR, Schweizer HP. 2005. A Tn7-based broad-range bacterial cloning and expression system. *Nature Methods* **2**: 443–448.

Deslandes L, Rivas S. 2012. Catch me if you can: bacterial effectors and plant targets. *Trends in Plant Science* **17**: 644–655.

Dreze M, Monachello D, Lurin C, Cusick ME, Hill DE, Vidal M, Braun P. 2010. High-quality binary interactome mapping. *Methods in Enzymology* **470**: 281–315.

Eitas TK, Nimchuk ZL, Dangl JL. 2008. Arabidopsis TAO1 is a TIR-NB-LRR protein that contributes to disease resistance induced by the *Pseudomonas syringae* effector AvrB. *Proceedings of the National Academy of Sciences, USA* **105**: 6475–6480.

Feng F, Zhou JM. 2012. Plant-bacterial pathogen interactions mediated by type III effectors. *Current Opinion in Plant Biology* **15**: 469–476.

Gimenez-Ibanez S, Hann DR, Ntoukakis V, Petutschnig E, Lipka V, Rathjen JP. 2009. AvrPtoB targets the LysM receptor kinase CERK1 to promote bacterial virulence on plants. *Current Biology* **19**: 423–429.

Gimenez-Ibanez S, Rathjen JP. 2010. The case for the defense: plants versus *Pseudomonas syringae*. *Microbes and Infection* **12**: 428–437.

Gohre V, Spallek T, Haweker H, Mersmann S, Mentzel T, Boller T, de Torres M, Mansfield JW, Robatzek S. 2008. Plant pattern-recognition receptor FLS2 is directed for degradation by the bacterial ubiquitin ligase AvrPtoB. *Current Biology* **18**: 1824–1832.

Guo M, Manulis S, Mor H, Barash I. 2002. The presence of diverse IS elements and an *avrPphD* homologue that acts as a virulence factor on the pathogenicity plasmid of *Erwinia herbicola* pv. *gypsophilae*. *Molecular Plant-Microbe Interactions* **15**: 709–716.

Guo M, Tian F, Wamboldt Y, Alfano JR. 2009. The majority of the type III effector inventory of *Pseudomonas syringae* pv. *tomato* DC3000 can suppress plant immunity. *Molecular Plant-Microbe Interactions* **22**: 1069–1080.

He P, Shan L, Lin NC, Martin GB, Kemmerling B, Nurnberger T, Sheen J. 2006. Specific bacterial suppressors of MAMP signaling upstream of MAPKKK in Arabidopsis innate immunity. *Cell* **125**: 563–575.

van Helden J, Andre B, Collado-Vides J. 2000. A web site for the computational analysis of yeast regulatory sequences. *Yeast* **16**: 177–187.

Jackson RW, Athanassopoulos E, Tsiamis G, Mansfield JW, Sesma A, Arnold DL, Gibbon MJ, Murillo J, Taylor JD, Vivian A. 1999. Identification of a pathogenicity island, which contains genes for virulence and avirulence, on a large native plasmid in the bean pathogen *Pseudomonas syringae* pathovar

phaseolicola. *Proceedings of the National Academy of Sciences, USA* **96**: 10875–10880.

Jamir Y, Guo M, Oh HS, Petnicki-Ocwieja T, Chen S, Tang X, Dickman MB, Collmer A, Alfano JR. 2004. Identification of *Pseudomonas syringae* type III effectors that can suppress programmed cell death in plants and yeast. *Plant Journal* **37**: 554–565.

Jones JD, Dangl JL. 2006. The plant immune system. *Nature* **444**: 323–329.

Karimi M, Inze D, Depicker A. 2002. GATEWAY vectors for *Agrobacterium*-mediated plant transformation. *Trends in Plant Science* **7**: 193–195.

Keen NT. 1990. Gene-for-gene complementarity in plant-pathogen interactions. *Annual Review of Genetics* **24**: 447–463.

Kim HS, Park BO, Yoo JH, Jung MS, Lee SM, Han HJ, Kim KE, Kim SH, Lim CO, Yun DJ *et al.* 2007a. Identification of a calmodulin-binding NAC protein as a transcriptional repressor in Arabidopsis. *Journal of Biological Chemistry* **282**: 36292–36302.

Kim HS, Park HC, Kim KE, Jung MS, Han HJ, Kim SH, Kwon YS, Bahk S, An J, Bae DW *et al.* 2012. A NAC transcription factor and SNI1 cooperatively suppress basal pathogen resistance in *Arabidopsis thaliana*. *Nucleic Acids Research* **40**: 9182–9192.

Kim SY, Kim SG, Kim YS, Seo PJ, Bae M, Yoon HK, Park CM. 2007b. Exploring membrane-associated NAC transcription factors in Arabidopsis: implications for membrane biology in genome regulation. *Nucleic Acids Research* **35**: 203–213.

Kim YS, Kim SG, Park JE, Park HY, Lim MH, Chua NH, Park CM. 2006. A membrane-bound NAC transcription factor regulates cell division in Arabidopsis. *Plant Cell* **18**: 3132–3144.

King EO, Ward MK, Raney DE. 1954. Two simple media for the demonstration of pyocyanin and fluorescin. *Journal of Laboratory and Clinical Medicine* **44**: 301–307.

Mishina TE, Zeier J. 2007. Bacterial non-host resistance: interactions of Arabidopsis with non-adapted *Pseudomonas syringae* strains. *Physiologia Plantarum* **131**: 448–461.

Monaghan J, Zipfel C. 2012. Plant pattern recognition receptor complexes at the plasma membrane. *Current Opinion in Plant Biology* **15**: 1–9.

Mukhtar MS, Carvunis AR, Dreze M, Epple P, Steinbrenner J, Moore J, Tasan M, Galli M, Hao T, Nishimura MT *et al.* 2011. Independently evolved virulence effectors converge onto hubs in a plant immune system network. *Science* **333**: 596–601.

Nanda AK, Andrio E, Marino D, Pauly N, Dunand C. 2010. Reactive oxygen species during plant-microorganism early interactions. *Journal of Integrative Plant Biology* **52**: 195–204.

Nelson BK, Cai X, Nebenfuhr A. 2007. A multicolored set of *in vivo* organelle markers for co-localization studies in Arabidopsis and other plants. *Plant Journal* **51**: 1126–1136.

Nicaise V, Roux M, Zipfel C. 2009. Recent advances in PAMP-triggered immunity against bacteria: pattern recognition receptors watch over and raise the alarm. *Plant Physiology* **150**: 1638–1647.

Ooka H, Satoh K, Doi K, Nagata T, Otomo Y, Murakami K, Matsubara K, Osato N, Kawai J, Carninci P *et al.* 2003. Comprehensive analysis of NAC family genes in *Oryza sativa* and *Arabidopsis thaliana*. *DNA Research* **10**: 239–247.

Puranik S, Sahu PP, Srivastava PS, Prasad M. 2012. NAC proteins: regulation and role in stress tolerance. *Trends in Plant Science* **17**: 369–381.

Ren T, Qu F, Morris TJ. 2000. HRT gene function requires interaction between a NAC protein and viral capsid protein to confer resistance to turnip crinkle virus. *Plant Cell* **12**: 1917–1925.

Ren T, Qu F, Morris TJ. 2005. The nuclear localization of the Arabidopsis transcription factor TIP is blocked by its interaction with the coat protein of Turnip crinkle virus. *Virology* **331**: 316–324.

Schulze S, Kay S, Buttner D, Egler M, Eschen-Lippold L, Hause G, Kruger A, Lee J, Muller O, Scheel D *et al.* 2012. Analysis of new type III effectors from *Xanthomonas* uncovers XopB and XopS as suppressors of plant immunity. *New Phytologist* **195**: 894–911.

Seo PJ, Kim MJ, Park JY, Kim SY, Jeon J, Lee YH, Kim J, Park CM. 2010. Cold activation of a plasma membrane-tethered NAC transcription factor induces a pathogen resistance response in Arabidopsis. *Plant Journal* **61**: 661–671.

Soon FF, Ng LM, Zhou XE, West GM, Kovach A, Tan MH, Suino-Powell KM, He Y, Xu Y, Chalmers MJ *et al.* 2012. Molecular mimicry regulates ABA signaling by SnRK2 kinases and PP2C phosphatases. *Science* **335**: 85–88.

Tian M, Chaudhry F, Ruzicka DR, Meagher RB, Staiger CJ, Day B. 2009. Arabidopsis actin-depolymerizing factor AtADF4 mediates defense signal transduction triggered by the *Pseudomonas syringae* effector AvrPphB. *Plant Physiology* **150**: 815–824.

Tsiamis G, Mansfield JW, Hockenhull R, Jackson RW, Sesma A, Athanassopoulos E, Bennett MA, Stevens C, Vivian A, Taylor JD *et al.* 2000. Cultivar-specific avirulence and virulence functions assigned to *avrPphF* in *Pseudomonas syringae* pv. *phaseolicola*, the cause of bean halo-blight disease. *EMBO Journal* **19**: 3204–3214.

Tsuda K, Katagiri F. 2010. Comparing signaling mechanisms engaged in pattern-triggered and effector-triggered immunity. *Current Opinion in Plant Biology* **13**: 459–465.

Tsuda K, Sato M, Glazebrook J, Cohen JD, Katagiri F. 2008. Interplay between MAMP-triggered and SA-mediated defense responses. *Plant Journal* **53**: 763–775.

Wang X, Basnayake BM, Zhang H, Li G, Li W, Virk N, Mengiste T, Song F. 2009. The Arabidopsis ATAF1, a NAC transcription factor, is a negative regulator of defense responses against necrotrophic fungal and bacterial pathogens. *Molecular Plant-Microbe Interactions* **22**: 1227–1238.

Wang Y, Li J, Hou S, Wang X, Li Y, Ren D, Chen S, Tang X, Zhou JM. 2010. A *Pseudomonas syringae* ADP-Ribosyltransferase inhibits Arabidopsis mitogen-activated protein kinase kinases. *Plant Cell* **22**: 2033–2044.

Wilton M, Subramaniam R, Elmore J, Felsensteiner C, Coaker G, Desveaux D. 2010. The type III effector HopF2Pto targets Arabidopsis RIN4 protein to promote *Pseudomonas syringae* virulence. *Proceedings of the National Academy of Sciences, USA* **107**: 2349–2354.

Winter D, Vinegar B, Nahal H, Ammar R, Wilson GV, Provart NJ. 2007. An "Electronic Fluorescent Pictograph" browser for exploring and analyzing large-scale biological data sets. *PLoS ONE* **2**: e718.

Wood JR, Vivian A, Jenner C, Mansfield JW, Taylor JD. 1994. Detection of a gene in pea controlling nonhost resistance to *Pseudomonas syringae* pv. *phaseolicola*. *Molecular Plant-Microbe Interactions* **7**: 534–537.

Yoon HK, Kim SG, Kim SY, Park CM. 2008. Regulation of leaf senescence by NTL9-mediated osmotic stress signaling in Arabidopsis. *Molecules and Cells* **25**: 438–445.

Zhang J, Lu H, Li X, Li Y, Cui H, Wen CK, Tang X, Su Z, Zhou JM. 2010. Effector-triggered and pathogen-associated molecular pattern-triggered immunity differentially contribute to basal resistance to *Pseudomonas syringae*. *Molecular Plant-Microbe Interactions* **23**: 940–948.

Zipfel C, Robatzek S, Navarro L, Oakeley EJ, Jones JD, Felix G, Boller T. 2004. Bacterial disease resistance in Arabidopsis through flagellin perception. *Nature* **428**: 764–767.

Zuo J, Niu QW, Chua NH. 2000. Technical advance: an estrogen receptor-based transactivator XVE mediates highly inducible gene expression in transgenic plants. *Plant Journal* **24**: 265–273.

Supporting Information

Additional supporting information may be found in the online version of this article.

Fig. S1 Immunoblots showing that transgenic Arabidopsis plants express HopD1-HA or NTL9$_{1\text{-}330}$-HA.

Fig. S2 No HR or ion leakage observed in the Arabidopsis *rpm1* mutant in response to bacterial strains.

Fig. S3 The first splice variant of *NTL9* is the dominant form in Arabidopsis.

Fig. S4 NTL9-regulated BZIP9 expression is repressed by ETI.

Fig. S5 GFP-NTL9 inside plant cells is not altered by the presence of HopD1-HA.

Fig. S6 HopD1 does not alter NTL9-dependent gene expression in the yeast one-hybrid system.

Table S1 Arabidopsis promoters that contain predicted NTL9 binding sites

Methods S1 Methods used for the data in the supporting information.

Please note: Wiley Blackwell are not responsible for the content or functionality of any supporting information supplied by the authors. Any queries (other than missing material) should be directed to the *New Phytologist* Central Office.